

Ultrafast carrier dynamics of InGaAsN and InGaAs single quantum wells

This content has been downloaded from IOPscience. Please scroll down to see the full text.

2008 J. Phys. D: Appl. Phys. 41 085107

(<http://iopscience.iop.org/0022-3727/41/8/085107>)

View [the table of contents for this issue](#), or go to the [journal homepage](#) for more

Download details:

IP Address: 140.113.38.11

This content was downloaded on 25/04/2014 at 16:21

Please note that [terms and conditions apply](#).

Ultrafast carrier dynamics of InGaAsN and InGaAs single quantum wells

Chih-Chang Hsu¹, Ja-Hon Lin², Ying-Shu Chen¹, Ying-Hsiu Lin¹,
Hao-Chung Kuo¹, Shing-Chung Wang¹, Wen-Feng Hsieh^{1,5},
Nelson Tansu³ and Luke J Mawst⁴

¹ Department of Photonics and Institute of Electro-Optical Engineering, National Chiao Tung University, 1001 Tahsueh Rd., Hsinchu 30050, Taiwan, Republic of China

² Department of Electro-Optical Engineering, National Taipei University of Technology, 1, Sec. 3, Chung-Hsiao E. Rd., Taipei 106, Taiwan, Republic of China

³ Center for Optical Technologies, Department of Electrical and Computer Engineering, Lehigh University, Bethlehem, PA 18015, USA

⁴ Reed Center for Photonics, Department of Electrical and Computer Engineering, University of Wisconsin-Madison, Madison, WI 53706, USA

E-mail: wfhsieh@mail.nctu.edu.tw

Received 22 October 2007, in final form 18 January 2008

Published 20 March 2008

Online at stacks.iop.org/JPhysD/41/085107

Abstract

Striking differences in differential reflectance and carrier relaxation in $\text{In}_{0.4}\text{Ga}_{0.6}\text{As}$ and $\text{In}_{0.4}\text{Ga}_{0.6}\text{As}_{0.98}\text{N}_{0.02}$ single quantum wells (SQWs) were studied using ultrafast time-resolved photoreflectance. Even with extremely thin SQW of only 60 Å within 3000 Å wide GaAs confining layers, negative and positive differential reflectance was observed for the excitation photon energy far above the bandgaps at 820 and 880 nm for both samples. Due to absorption by the GaAs confining layer, the peak differential reflectance pumped at 820 nm is an order of magnitude larger than that pumped at 880 nm; and it is larger for InGaAs SQWs than for InGaAsN SQWs. The shorter carrier lifetimes of these samples result from carrier–carrier scattering as pumped at both wavelengths. The longer carrier lifetime as pumped at 880 nm is due to hot phonon decay in InGaAs but may be due to stimulated emission in InGaAsN. The results reveal that the carrier dynamics is strongly affected by N incorporation that causes local defects in InGaAsN SQWs to reduce the carrier relaxation.

1. Introduction

InGaAsN/GaAs heterostructures have attracted much interest because of their large bandgap shifting upon nitrogen incorporation [1] and their potential for long wavelength photonic device applications [2–4]. The large band offsets are due to large electronegativity of N atoms which pulls down both conduction and valence band edges in the InGaAsN quaternary alloy and leads to better electron confinement. As a result, better temperature performance than the conventional InP-based materials can be achieved [5, 6]. Recently, high-performance, such as very low threshold and transparency current density and high current injection efficiency, strain-compensated InGaAsN quantum-well (QW) lasers that extend the lasing emission wavelength to 1300 nm

at room temperature have been realized by Tansu and co-workers [7–9].

The carrier relaxation processes in the semiconductor lasers that had been widely investigated crucially affected the laser characteristics and performance [10–14]. The dynamics of carrier recombination for InGaAs(N) single quantum wells (SQWs) have been investigated by using time-resolved photoluminescence (TRPL) measurements [10–12]. The low temperature TRPL measurements showed that the localization of carriers arising from alloy fluctuations upon nitrogen incorporation channels the carrier decay via nonradiative recombination processes. Therefore, the lifetime of radiative recombination is shortened. In addition, carrier recombination was investigated by comparing the differential carrier lifetimes on two $\text{InGaAs}_{1-x}\text{N}_x$ SQW laser diodes that have different nitrogen contents x in the well [13]. It showed that the recombination lifetime is significantly reduced from 10 to 1 ns

⁵ Author to whom any correspondence should be addressed.

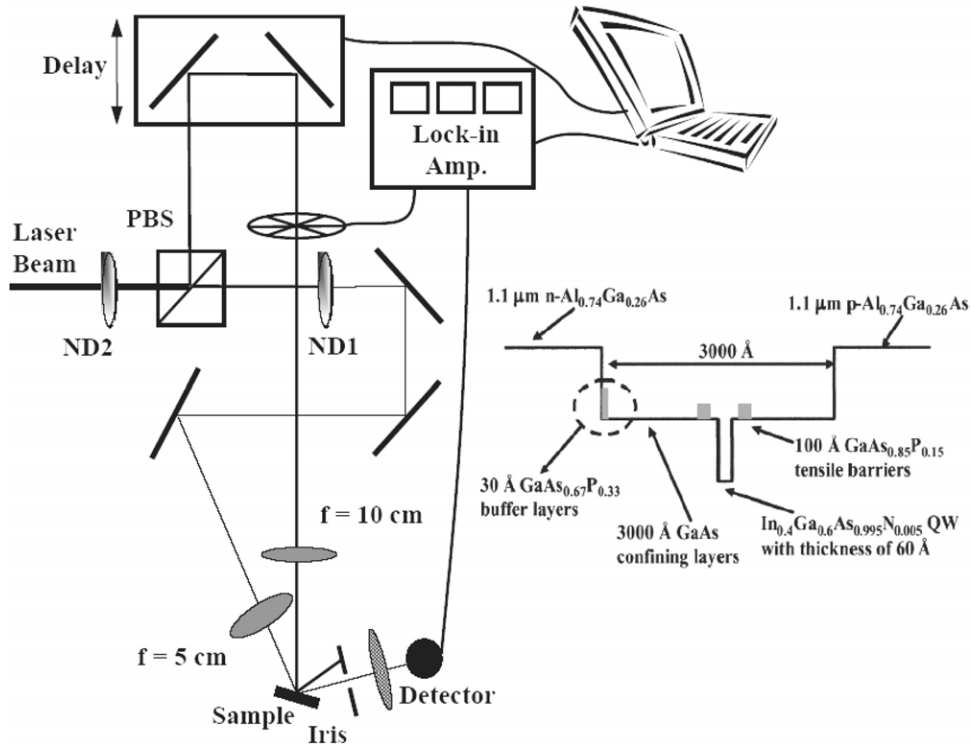


Figure 1. The schematic diagram of the ultrafast time-resolved photoreflectance experiment. The inset shows the schematic energy band diagram for the InGaAs(N) SQW laser structure.

when nitrogen is added into the QW. These samples reveal an enhancing quantum-dot (QD) like behaviour with strong localization as increasing nitrogen content that affects the carrier dynamics [14].

Prior to carrier recombination, there are various microscopic processes of momentum and energy relaxation of carriers in the semiconductors such as carrier–carrier scattering, optical-phonon scattering, intervalley scattering and Auger recombination, which occur in the femtosecond (fs) to picosecond (ps) time scale after optical or electrical excitation of carriers. In order to investigate such a short interaction time, fs pump–probe measurements, including differential transmission, reflection and absorption spectroscopies using ultrashort pulse lasers as exciting sources, have been widely used for III–V semiconductors [15, 16]. Some experimental results of InGaAs QWs by using the pump–probe technique have been reported [17–19]. Sucha *et al* presented time-resolved measurements of carrier dynamics in bulk and QW InGaAs using differential absorption spectroscopy [17]. They found that the carrier thermalization time is about 200–300 fs in spite of the well width ranging from 100 to 6000 Å. Borri *et al* studied the temperature and the density dependences of exciton dephasing time in an $\text{In}_{0.18}\text{Ga}_{0.82}\text{As}/\text{GaAs}$ SQW by a time-integrated four-wave mixing [18]. They found that the acoustic-phonon coefficient increases by increasing the well width and the optical-phonon coefficient shows a nonsystematic dependence on the well width compared with bulk GaAs. Bhattacharya *et al* performed pump–probe differential transmission spectroscopy on $\text{In}_{0.4}\text{Ga}_{0.6}\text{As}/\text{GaAs}/\text{AlGaAs}$ QD lasers and found that the relaxation time of these carriers to the QD ground state is longer

than 100 ps [19]. However, to the best of our knowledge, there are no reports on the effect of N incorporation on the ultrafast carrier dynamics of $\text{InGaAs}_{1-x}\text{N}_x$ SQWs. In this paper, we report the ultrafast time-resolved photoreflectance of $\text{In}_{0.4}\text{Ga}_{0.6}\text{As}_{1-x}\text{N}_x/\text{GaAs}$ SQWs with and without N incorporation.

2. Experimental details

The $\text{In}_{0.4}\text{Ga}_{0.6}\text{As}_{1-x}\text{N}_x$ SQW structures studied here having N composition $x = 0\%$ (InGaAs) and 2% (InGaAsN) were grown by low-pressure metal-organic chemical vapour deposition (LP-MOCVD) [7]. The schematic energy band diagram [7] is shown in the inset of figure 1. A 60 Å $\text{In}_{0.4}\text{Ga}_{0.6}\text{As}_{1-x}\text{N}_x$ SQW as the active region is surrounded by tensile-strain barriers of $\text{GaAs}_{0.85}\text{P}_{0.15}$ on each side with 100 Å spacing that improved optical luminescence for highly compressively strained InGaAs(N) QW. The tensile buffer for this structure consists of a 30 Å $\text{GaAs}_{0.67}\text{P}_{0.33}$ layer. Finally, the overall 3000 Å GaAs confining layer is sandwiched by the lower and top cladding layers of the QW structure, consisting of $\text{Al}_{0.74}\text{Ga}_{0.26}\text{As}$ layers for both n- and p-cladding layers. Using the cleaved edges as reflection mirrors for the QW structures under electric bias, the characteristics of lasers for $\text{In}_{0.4}\text{Ga}_{0.6}\text{As}_{1-x}\text{N}_x$ SQWs were shown in [7, 20].

The ultrafast time-resolved photoreflectance experiment is schematically shown in figure 1. The measurement is performed at room temperature with the use of a self-mode-locked Ti:sapphire laser (Coherent Mira900) operated with centre wavelengths of 820 nm (photon energy of 1.51 eV) and 880 nm (1.41 eV) separately with a pulse repetition rate

of 75 MHz and a pulse width of 230 fs. The laser beam was first split into pump and probe beams by a polarization beamsplitter (PBS) to minimize the optical coherent artefact from the scattered pump beam. The variable neutral density filter (ND1) was used to attenuate the power of the probe beam such that the pump–probe ratio is maintained at 160 : 1. Another variable neutral density filter (ND2) was put ahead of the PBS to adjust the incident power and to keep a constant pump–probe ratio. A mechanical chopper is used to chop the pump beam; the change in the reflected probe intensity induced by the pump is a function of the time delay between the pump and probe pulses. The minimum time delay is 8.33 fs for a translation stage with 1.25 μm resolution. The pump and probe beams were separately focused by two convex lenses with focal lengths of 10 cm and 5 cm, corresponding to focusing areas of 300 μm^2 and 75 μm^2 , respectively, on the tested samples without electric bias. The spatial overlap of the pump and probe beams on the sample was monitored by a CCD camera to ensure that the probe beam is located within the centre of the pump beam. We used an iris to block the reflected pump beam, and the reflected probe beam was detected by a silicon photodetector (Hamamatsu C5460) and then connected to a lock-in amplifier (Stanford Research System, Model SR830). The signal was finally recorded on a personal computer as a function of temporal delay between the pump and probe beams with the pump power being varied from 10 to 60 mW corresponding to the peak intensity of the pump pulse from 193 to 1159 MW cm^{-2} or the incident fluence from 0.44 to 2.67 J m^{-2} , which is in the low fluence regime ($F < 0.5 \text{ kJ m}^{-2}$) for GaAs as described in [2].

3. Results and discussion

Although the well width of the SQWs is only 60 \AA within a 3000 \AA wide GaAs confining layer (bandgap $E_g \sim 1.42 \text{ eV}$), we still observed quite different time-resolved photoreflectance from InGaAs and InGaAsN SQWs as the pumping power varies from 10 to 50 mW at a wavelength of 820 nm, shown in figure 2, can still be discriminated. For comparison, we also showed the results of bulk GaAs in figure 2(a) which was pumped at 50 mW; we found, in contrast to the positive change in transient reflectance ($\Delta R/R$) from bulk GaAs, a negative $\Delta R/R$ from both SQWs in figures 2(b) and (c). The positive change in the measured reflection ($\Delta R > 0$) in bulk GaAs is mainly due to the band filling effect, indicating a positive change in the refractive index ($\Delta n > 0$) [22]. Since the pump photon energy (1.51 eV) is slightly larger than the bandgap of bulk GaAs, the measured result of bulk GaAs agrees with that of [22]. The rise in the reflectance of bulk GaAs is initially due to the generation of carriers occupying the optical-coupled transition states, and the decay is due to carriers being scattered out of their initial states and subsequent relaxing towards the band edges. On the other hand, the bandgaps of InGaAs and InGaAsN SQWs determined from room-temperature PL spectra (not shown here) are consistent with the previous reports [9, 23] of 1.04 eV (1.2 μm) and 0.86 eV (1.45 μm), respectively. Due to the much smaller bandgap energy compared with pump photo energy,

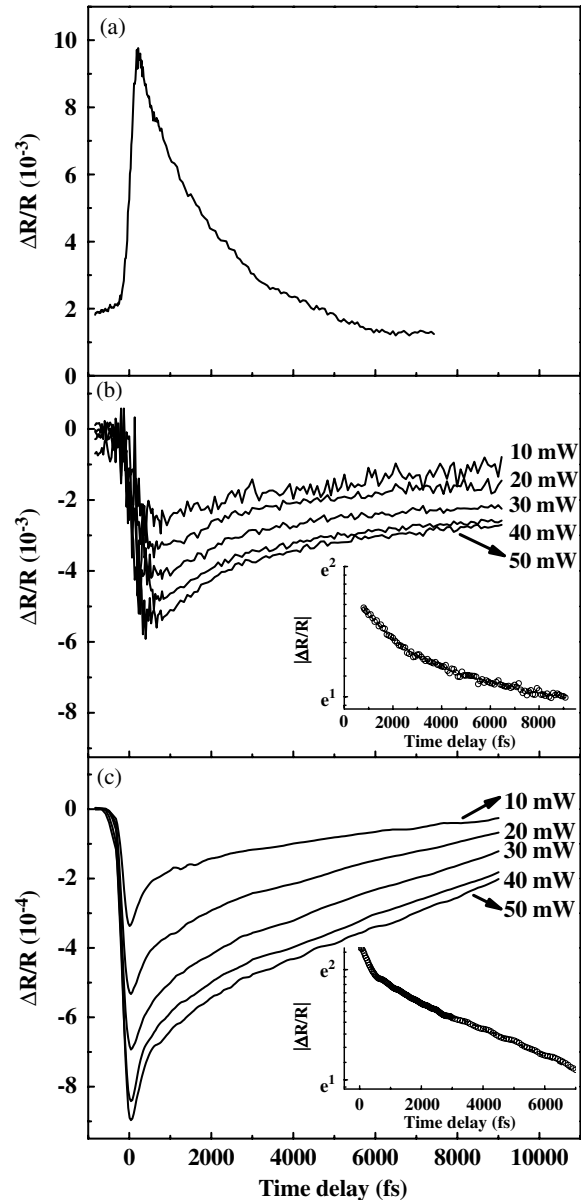


Figure 2. The time-resolved photoreflectance of (a) bulk GaAs (50 mW pumped) and varying pump powers for (b) $\text{In}_{0.4}\text{Ga}_{0.6}\text{As}$ SQW and (c) $\text{In}_{0.4}\text{Ga}_{0.6}\text{As}_{0.98}\text{N}_{0.02}$ SQW at the pumping wavelength of 820 nm. The inset shows the data pumped at 50 mW on the semi-log scale and the dashed line is the fitting curve.

the band filling could not contribute to the index change. Furthermore, because the pump photon energy is much larger than the energy shift due to bandgap renormalization, which usually gives less than 1 meV, the negative index change resulting from bandgap renormalization should be negligible. The negative change in transient reflectance for InGaAs and InGaAsN SQW samples could result from either free carrier absorption [24] or re-excitation of trapped carriers into the conduction band [22]. But the thickness of these QWs is only 60 \AA and the pumping photon energy is above the bandgap of the GaAs confining layer; we speculate that parts of carriers are mainly excited in the confining layer and then quickly trapped into the QWs of both InGaAs and InGaAsN SQW samples.

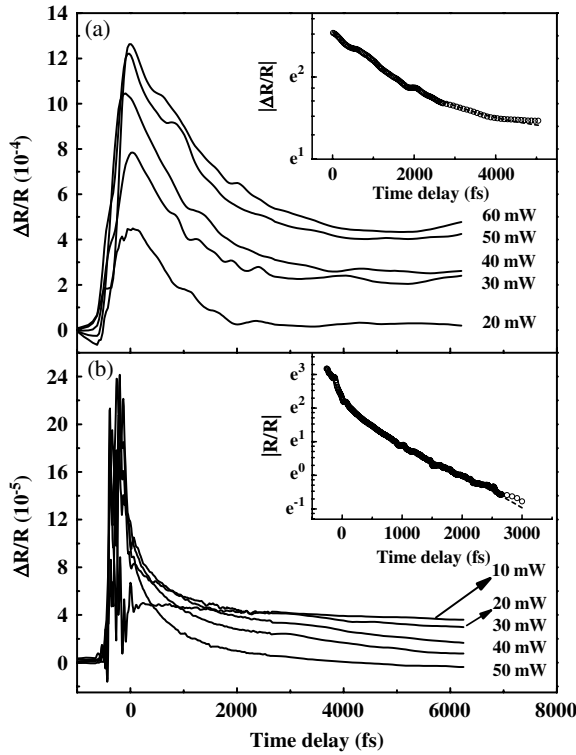


Figure 3. The time-resolved photoreflectance of varying pump powers for (a) $\text{In}_{0.4}\text{Ga}_{0.6}\text{As}$ SQW and (b) $\text{In}_{0.4}\text{Ga}_{0.6}\text{As}_{0.98}\text{N}_{0.02}$ SQW at the pumping wavelength of 880 nm. The inset shows the data pumped at 50 mW on the semi-log scale and the dashed line is the fitting curve.

We then tuned the laser wavelength to 880 nm which is just below the bandgap of GaAs but remains above the bandgap of InGaAs and InGaAsN SQWs. Figure 3 shows the results of time-resolved photoreflectance of InGaAs and InGaAsN SQWs with the pumping power varying from 10 to 60 mW at the wavelength of 880 nm. Notice that the measured ΔR had turned to positive. The opposite phenomenon with respect to 820 nm pumping may result from different initial occupied states of the photoexcited carriers at two pump wavelengths. Based on the absorption curve of bulk GaAs presented in [25], we estimated the penetration depths of GaAs at 820 nm and 880 nm to be $1.43 \mu\text{m}$ and $1000 \mu\text{m}$, respectively. When the samples were pumped by 820 nm light, nearly 20% of the incident intensity was absorbed while passing through the $0.3 \mu\text{m}$ thick GaAs confining layer and then absorbed by the SQWs. However, when pumped at 880 nm, the pump beam can pass directly through the GaAs confining layer with extremely low absorption ($<0.05\%$) and can efficiently excite the carriers in the QW. Therefore, as the pumping wavelength is 880 nm, carriers are mainly generated in the 60 \AA QW, and then quickly fill up the conduction and the valence bands. The positive change in the transient reflectance is due to the band filling effect, indicating a positive change in the refractive index ($\Delta n > 0$) [26].

The absolute peak magnitude of $\Delta R/R$ is proportional to the carrier density accumulated in the allowed optical transition states after photoexcitation. Figure 4 shows the peak magnitudes of $|\Delta R/R|$ of an InGaAs SQW (■) and an

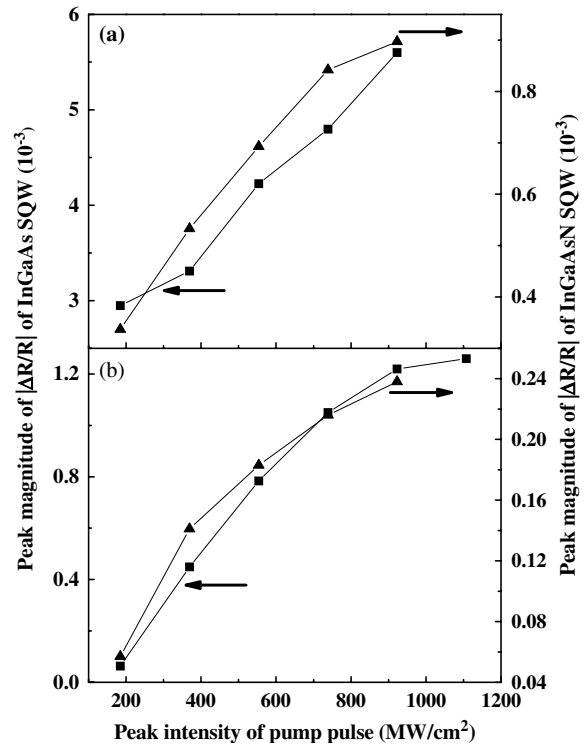


Figure 4. Peak magnitude of $|\Delta R/R|$ of $\text{In}_{0.4}\text{Ga}_{0.6}\text{As}$ SQW and $\text{In}_{0.4}\text{Ga}_{0.6}\text{As}_{0.98}\text{N}_{0.02}$ SQW with various peak intensities of the pump pulse at pumped wavelengths of (a) 820 nm and (b) 880 nm. Symbols (■) and (▲) represent InGaAs and InGaAsN SQWs, respectively.

InGaAsN SQW (▲) versus the peak intensity of the pump pulse at pumped wavelengths of (a) 820 nm and (b) 880 nm, respectively. The peak magnitudes of $|\Delta R/R|$ of both samples increase with the peak intensity of the pump pulse when the pump wavelength is 820 nm, as shown in figure 4(a). Due to absorption by the GaAs confining layer, $|\Delta R/R|$ pumped at 820 nm is an order of magnitude larger than that pumped at 880 nm but a larger $|\Delta R/R|$ for InGaAs SQW than that for InGaAsN SQW. It is worth noting that when pumped at 880 nm, whose photon energy is below the GaAs bandgap but above those of both SQWs, the peak magnitude of $|\Delta R/R|$ of the InGaAs SQW increases faster than that of the InGaAsN SQW with increasing peak intensity of the pump pulse. After being pumped to the higher states, the carriers may diffuse into the 3000 \AA GaAs confining layer or be trapped by the local trapped states in a QW. The band filling effect is not obvious, so that $|\Delta R/R|$ basically increases with the pumping power for those pumping at a wavelength of 820 nm. However, when pumping at 880 nm, carriers will localize in the InGaAs(N) SQW. The band filling effect dominates to cause positive Δn that will be saturated at high pumping. Therefore the relations of peak magnitude of $|\Delta R/R|$ versus the peak intensity of the pump pulse are nonlinear as shown in figure 4(b).

The carrier relaxation times are extracted from fitting the normalized $\Delta R/R$ traces of figures 2 and 3 by using a double exponential function $A \exp(-t/\tau_1) + B \exp(-t/\tau_2)$. The insets of figures 2 and 3 in the semi-log scale are the profiles pumped at 50 mW which show an initial fast decay followed by a

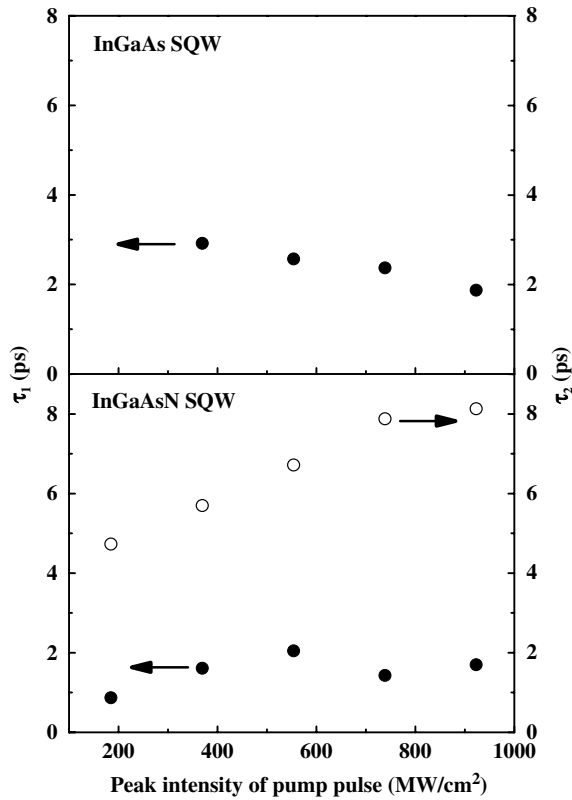


Figure 5. The carrier lifetime versus peak intensity of the pump pulse in InGaAs and InGaAsN SQWs with the pump wavelength at 820 nm. The (●) and (○) symbols present the carrier lifetimes τ_1 and τ_2 , respectively.

slower relaxation. The fitting results are shown in figures 5 and 6. In the InGaAsN SQW, the photoexcited carrier could be trapped by the local defects more quickly and efficiently than in the InGaAs SQW due to N incorporation during or after they experienced inelastic scattering to lose their excess kinetic energy. All of τ_2 for the InGaAs SQW pumped with various powers at 820 nm are longer than the measured time delay window (9 ps) which may be unconvincing; therefore, we did not include these data in figure 5 and will discuss only the carrier lifetime τ_1 for the InGaAs SQW which approximates 2–3 ps. For the InGaAsN SQW the fast lifetime τ_1 approximates 1–2 ps and the slow one τ_2 approximates 5–8 ps with a pumping wavelength of 820 nm. Both the carrier lifetimes τ_1 of the InGaAs SQW and the InGaAsN SQW are almost constant on increasing the peak intensity of the pump pulse and those are attributed to carrier–carrier scattering. Because the pumping photon energy still remains, the rate of carrier–carrier scattering will basically not change even if the pumping power is already different. The carrier lifetime τ_2 of InGaAsN on increasing the pumping power is attributed to hot phonon decay [26]. After receiving the energy from the pumping beam, the carriers transfer their additional kinetic energy to phonons. These phonons become hot and then transfer their energy back to the carriers. As a result, carriers which have more kinetic energy also take more time to relax to thermalization and a longer time to decay when the pumping power is rising.

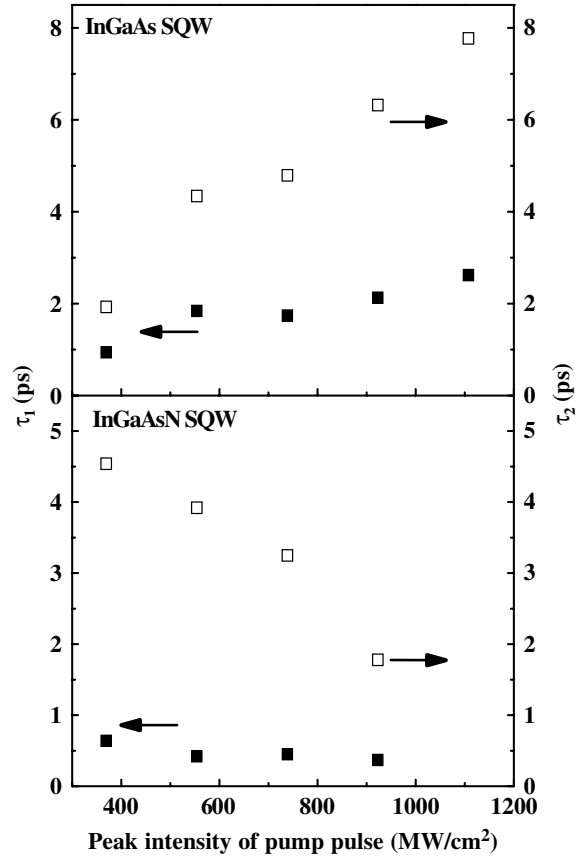


Figure 6. The carrier lifetime versus peak intensity of the pump pulse in InGaAs and InGaAsN SQWs with the pump wavelength at 880 nm. The (■) and (□) symbols present the carrier lifetimes τ_1 and τ_2 , respectively.

Figure 6 shows that the fast carrier lifetimes τ_1 of InGaAs and InGaAsN SQWs are approximately 1–2.5 ps and 0.3–0.8 ps with the pumping wavelength adjusted to 880 nm. The τ_1 of both samples is almost unchanged with increasing peak intensity of the pump pulse which is again due to mainly the carrier–carrier scattering occurring at this moment. The longer component τ_2 of InGaAs increases from 2 to 8 ps with increasing pumping power also resulting from hot phonons. However, τ_2 of InGaAsN decreases from 4.5 to 2 ps as the pumping power increases which may result from stimulated emission. On stronger pumping intensity, more carriers will be in the upper state, and stimulated emission [27] or Auger recombination [28, 29] will quickly bring the carriers to the valence band to cause faster carrier decay. Generally, the order of carrier density and time scale for Auger recombination were 10^{20} cm^{-3} and 10^{-10} s , respectively [21]. However, the order of carrier density of the GaAs bulk, 50 mW pumped at 820 nm as shown in figure 2(a), evaluated on the basis of the Drude model [30, 31] was 10^{18} cm^{-3} , and the carrier lifetimes of InGaAsN were less than 10 ps; therefore, we believe stimulated emission is the dominant mechanism.

Comparing InGaAs SQW with InGaAsN SQW clearly reveals that the former one shows not only an order of magnitude $\Delta R/R$ larger than the latter one but also a longer relaxation time. This is consistent with the time-resolved PL measurements done by Lifang *et al* [14]

and the below threshold modulation frequency response measurements studied by Anton *et al* [13]. This phenomenon can be explained by the presence of defects after nitrogen incorporation. Some trap states are formed within the bandgap by defects, and they will efficiently capture excited carriers. The electrons in the conduction band can also be trapped by spatially localized states resulting from alloy fluctuation. The trap states act like nonradiative recombination centres. This process lasts a shorter time than the intraband relaxation, and that is why the carrier lifetime in InGaAsN is shorter.

4. Conclusion

We have studied ultrafast time-resolved photoreflectance of InGaAs_{1-x}N_x ($x = 0$ and 2%) SQWs. Even with an extremely thin SQW of only 60 Å within 3000 Å wide GaAs confining layers, we found striking differences in the differential reflectance and the carrier relaxation in InGaAs and InGaAsN SQWs for pumping at 820 and 880 nm. The origin of negative differential reflectance is due to either free carrier absorption or re-excitation of trapped carriers into the conduction band that results from the carriers generated in the GaAs confining layer which were then trapped into the QWs for the excited photon energy far above the bandgaps of GaAs. The positive change in transient reflectance is due to the band filling effect when the pumped wavelength is 880 nm. With pumping wavelengths at 820 and 880 nm, the shorter carrier lifetimes of InGaAs and InGaAsN SQWs are both independent of the pumping power, which indicates the mechanism of carrier-carrier scattering. Nevertheless, the longer lifetime is proportional to the pumping power due to hot phonon decay in the InGaAs SQW and inversely proportional to the pumping power due to stimulated emission in the InGaAsN SQW with the pumping wavelength at 880 nm. Most importantly, the carrier lifetime in the InGaAsN SQW is shorter than that in the InGaAs SQW, which accounts for the appearance of local defect states during nitrogen doping.

Acknowledgments

This research was partially supported by the National Science Council (NSC), Taiwan, under Grants NSC 96-2628-M-009-001-MY3 and 96-2628-E-009-018-MY3.

References

- [1] Shan W, Waluskiewicz W, Ager J W III, Haller E E, Geisz J F, Friendmann D J, Olson J M and Kurtz S R 2002 *Phys. Rev. Lett.* **82** 1221
- [2] Ellmers C, Hohnsdorf F, Koch J, Agert C, Leu S, Karaiskaj D, Hofmann M, Stolz W and Ruhle W W 1999 *Appl. Phys. Lett.* **74** 2271
- [3] Tansu N, Yeh J Y and Mawst L J 2003 *IEEE J. Sel. Top. Quantum Electron.* **9** 1220
- [4] Yeh J Y, Tansu N and Mawst L J 2004 *Electron Lett.* **40** 739
- [5] Kondow M, Uomi K, Niwa A, Kitatani T, Watahiki S and Yazawa Y 1996 *Japan. J. Appl. Phys.* **35** 1273
- [6] Xin H P and Tu C W 1998 *Appl. Phys. Lett.* **72** 2442
- [7] Tansu N, Kirsch N J and Mawst L J 2002 *Appl. Phys. Lett.* **81** 2523
- [8] Tansu N, Yeh J Y and Maest L J 2003 *Appl. Phys. Lett.* **82** 3008
- [9] TaOnsu N, Yeh J Y and Maest L J 2003 *Appl. Phys. Lett.* **82** 4038
- [10] Mair R A, Lin J Y, Jiang H X, Jones E D, Allerman A A and Kurtz S R 2000 *Appl. Phys. Lett.* **76** 188
- [11] Kaschner A, Lüttgert T, Born H, Hoffmann A, Egorov A Yu and Riechert H 2001 *Appl. Phys. Lett.* **78** 1391
- [12] Vinattieri A, Alderighi D, Zamfirescu M, Colocci M, Polimeni A, Capizzi M, Gollub D, Fischer M and Forchel A 2003 *Appl. Phys. Lett.* **82** 2805
- [13] Anton O, Menoni C S, Yeh J Y, Mawst L J, Pikal J M and Tansu N 2005 *IEEE Photon. Technol. Lett.* **17** 953
- [14] Xu Lifang, Patel D, Vaschenko G, Anton O, Menoni C S, Yeh J Y, Roy T T V, Mawst L J and Tensu N 2005 *Proc. Conf. on Lasers and Electro-Optics (Baltimore, MD)* (Optical Society of America) CFE4
- [15] Auston D H, McAfee S, Shank C V, Ippen E P and Teschke O 1978 *Solid-State Electron.* **21** 147
- [16] Lin W Z, Schoenlein R W, Ippen E P and Logan R A 1987 *Appl. Phys. Lett.* **50** 124
- [17] Sucha G, Bolton S R, Chemla D S, Sivco D L and Cho A Y 1994 *Appl. Phys. Lett.* **65** 1486
- [18] Borri P, Langbein W, Hvam J M and Martelli F 1999 *Phys. Rev. B* **59** 2215
- [19] Bhattacharya P, Ghosh S, Pradhan S, Singh J, Wu Z K, Urayama J, Kim K and Norris T B 2003 *IEEE J. Quantum Electron.* **39** 952
- [20] Tansu N and Mawst L J 2002 *IEEE Photon. Technol. Lett.* **14** 444
- [21] Tsen K T 2001 *Ultrafast Physical Processes in Semiconductors* (San Diego, CA: Academic) p 178
- [22] Bennett B R, Soref R A and Del Alamo J A 1990 *IEEE J. Quantum Electron.* **26** 113
- [23] Lai F I *et al* 2005 *Japan. J. Appl. Phys.* **44** 6204
- [24] Siegner U, Fluck R, Zhang G and Keller U 1996 *Appl. Phys. Lett.* **69** 2566
- [25] Wilson J and Hawkes J 1998 *Optoelectronics: An Introduction* (London: Prentice Hall Europe)
- [26] Shah J 1996 *Ultrafast Spectroscopy of Semiconductors and Semiconductor Nanostructures* (Berlin: Springer)
- [27] Ozgur U and Everitt H O 2003 *Phys. Rev. B* **67** 155308
- [28] Hader J, Moloney J V and Koch S W 2005 *IEEE J. Quantum Electron.* **41** 1217
- [29] Andreev A D and O'Reilly E P 2004 *Appl. Phys. Lett.* **84** 1826
- [30] Esser A, Kutt W, Strahlen M, Maidorn G and Kurz H 1999 *Appl. Surf. Sci.* **46** 446
- [31] Tan H W, van Driel H M, Schweizer S L, Wehrspohn R B and Gosele U 2004 *Phys. Rev. B* **70** 205110